JACS
JOURNAL OF THE AMERICAN CHEMICAL SOCIETY

ARTICLE

pubs.acs.org/JACS

Electron Donor−Acceptor Interactions with Flanking Purines Influence the Efficiency of Thymine Photodimerization

Zhengzheng Pan, Mahesh Hariharan,† Joshua D. Arkin, Almaz S. Jalilov, Martin McCullagh, George C. Schatz,* and Frederick D. Lewis*

Department of Chemistry, Northwestern University, Evanston, Illinois 60208-3113, United States

Supporting Information

ABSTRACT: Quantum yields for thymine photodimerization (Φ_{TT}) have been determined for a series of short DNA single-strand and base-paired hairpin structures possessing a single thymine−thymine step with flanking purines. Values of Φ_{TT} are strongly dependent upon the oxidation potential of the flanking purine, decreasing in the order: inosine > adenine > guanine > deazaguanine. The dependence of Φ_{TT} on the ionization potential of the flanking purine is more pronounced when the purine of lower oxidation potential is located at the 5′- versus 3′-position in either a single strand or a hairpin. Molecular dynamics simulations for hairpin structures indicate that the TT step is π-stacked with both the 5′ and 3′ purine, but that there is little π-stacking with either purine in single-strand structures. The observation of moderately intense long-wavelength UV absorption features for hairpins having 5′-Z or G flanking purines suggests that excitation of ground state donor−acceptor complexes may account for more extensive quenching of dimerization by 5′- versus 3′-purines. The "purine effect" on Φ_{TT} is attributed to a combination of ground state conformation, ground state electron donor−acceptor interactions, and excited state exciplex formation.

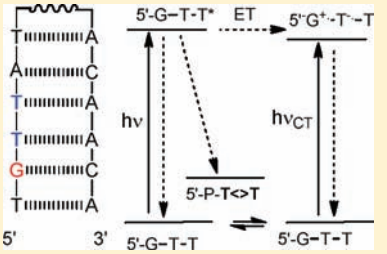

INTRODUCTION

Ultraviolet irradiation of cellular DNA results in the formation of several pyrimidine photodimers, the most prevalent of which is the *cis*−*syn* thymine (2 + 2) dimer T<>T formed via the (2 + 2) cycloaddition reaction of adjacent thymines (Chart 1a).[1] The formation of pyrimidine photodimers is a leading cause for the development of nonmelanoma skin cancers and thus has been the object of continuing interest for over five decades.[2] Femtosecond time-resolved IR studies of TT dimerization in the dinucleotide T_pT and oligonucleotide dT_{18} have shown that dimerization is complete within 1 ps.[3,4] However, the quantum yields for dimerization are low both in model systems (0.013 for T_pT)[5] and in native DNA (Φ_{TT} < 0.03).[6] The seeming dichotomy between ultrafast dimerization rate and low efficiency has been attributed to ground state conformational control of dimerization efficiency (Scheme 1).[7−9] As a consequence of ultrafast decay of the thymine singlet state, only ground state conformers of T_pT that have well-aligned double bonds and appropriate interbond separation can undergo photodimerization in competition with nonradiative decay.

Both the relative efficiency and distribution of products obtained from pyrimidine dimerization are known to be dependent upon the DNA base sequence, higher yields being observed for TT steps having pyrimidine versus purine flanking bases.[10] The effects of flanking purine structure (Chart 1b) on the relative yields of T<>T formation in duplex systems possessing a single TT or T-^{m}C step (^{m}C = 5-methylcytosine) have been the subject of several recent investigations.[11−13] Significantly lower yields were observed for flanking guanine (G) versus adenine (A) bases, the guanine effect being larger for a 5′G versus 3′G both in duplex and in single-strand systems. Lower yields for flanking deazaguanine (Z)[12] and higher yields for flanking inosine (I)[13] were associated with changes in the purine ionization potential. Factors which have been suggested to contribute to the effects of purines on relative yield include increased duplex rigidity for flanking GC versus AT base pairs,[11] excited state electron-transfer-sensitized dimer repair,[12] and quenching of dimerization via electron transfer from the flanking purine to excited T.[13] Curiously, a possible role for ground state donor−acceptor interactions between π-stacked purine and thymine bases has not been considered.

In view of the diverse nature of these explanations and the absence of quantitative data, the dependence of TT dimerization efficiency (quantum yields) on ground state conformation, and purine ionization potential, we have undertaken an investigation of the purine effect in the single-strand and hairpin systems shown in Chart 1c. The two-letter codes for these systems refer to the flanking purines X and Y and the subscripts S and H designate single-strand and hairpin (double strand) systems. These systems possess a single TT step located in the middle of a hexanucleotide sequence with the purines A, G, Z, and I (Chart 1b) in the flanking positions.

RESULTS

Synthesis and Characterization. The synthesis and characterization of the single-strand and hairpin systems AA_S and AA_H

Received: June 13, 2011
Published: October 27, 2011

   dx.doi.org/10.1021/ja205460f | J. Am. Chem. Soc. 2011, 133, 20793–20798

Chart 1. Structures of (a) the *cis*−*syn* Dimer T<>T, (b) Thymine and the Purine Bases, and (c) Single-Strand (S) and Hairpin (H) Sequences[a]

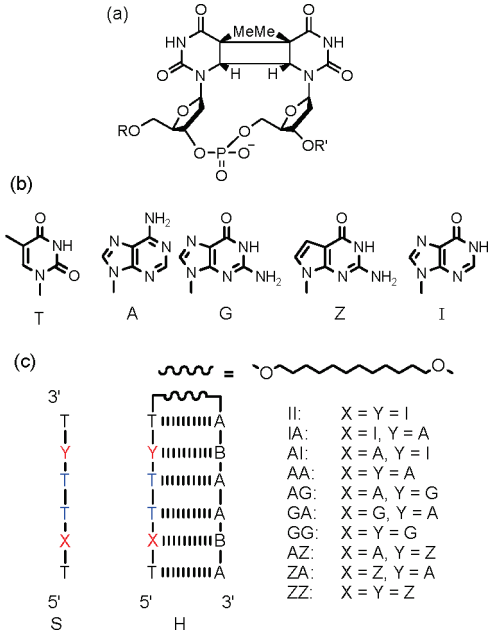

[a]The complementary base for G, Z, and I is cytosine.

Scheme 1. Ground State Conformational Control of TT Photodimerization

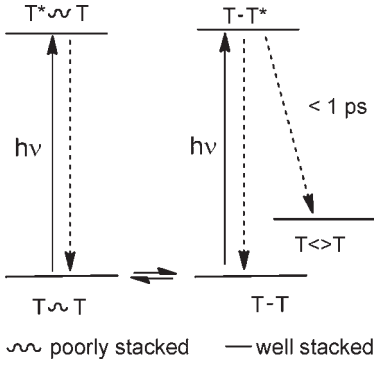

have been reported.[14,15] Similar procedures were employed for the other systems in Chart 1c. MALDI-TOF spectral data for single-strand and hairpin systems and melting temperatures for the hairpins are reported as Supporting Information (Table S1). The hairpin melting temperatures follow the trend (G ~ Z > A > I) with a lowest value of T_m 43.5 °C for II_H.

Conformational modeling using the CHARMM force field[16] to obtain probability densities for the distance separating the midpoints of the TT double bonds has previously been reported for AA_S and AA_H.[17] Probability densities for TT stacking in the hairpin systems AG_H and GA_H are shown in Figure S1 along with the results for AA_H. All three hairpins have similar probability densities. Similar results were obtained for the corresponding single-strand systems AA_S, AG_S, and GA_S.

Pairwise TT and AT probability distributions obtained from multiple snapshots for AA_S and AA_H are shown in Figure 1,

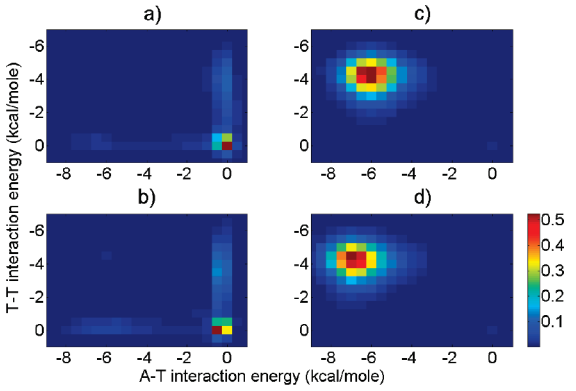

Figure 1. Pairwise TT and AT probability densities for the TT step with the adjacent 5′-A in (a) AA_S and (c) AA_H and the 3′-A in (b) AA_S and (d) AA_H. More negative energies indicate stronger interaction.

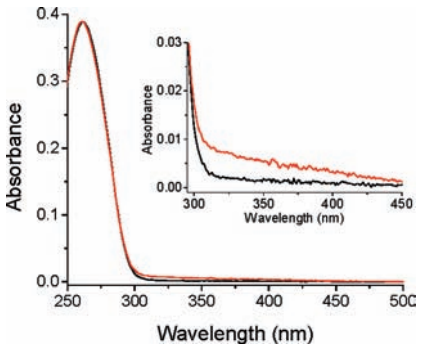

Figure 2. UV spectrum of ca. 3 μM GA_H (red) and AG_H (black) in 10 mM phosphate buffer (pH 7.1) containing 100 mM NaCl.

in which more negative energies correspond to stronger base−base interactions. The probability of either strong TT or AT interaction in the single-strand system is low and the probability of ATT or TTA interaction is too low to be detected visually (Figure 1a,b). In contrast, the probabilities of ATT and TTA interactions are high in the hairpin systems (Figure 1c,d). We note that the average interaction energy for TTA is slightly larger than for ATT.

The UV spectra of both single-strand and hairpin systems display a single maximum around 260 nm with a weak tail extending to wavelengths longer than 300 nm. Typical spectra are shown in Figure 2, and Figures S2 and S3. The spectrum of GA_H has a stronger tail than that of AG_H (Figure 2) as does that of ZA_H versus AZ_H (Figure S2) and AA_H versus AA_S (Figure S3). The molar absorption coefficient of AA_H at 350 nm (ε_{350}) is 76 M^{-1} s^{-1} or 12 M^{-1} s^{-1} per base pair. Substitution of G or Z for A at the 5′-position results in a large increase in ε_{350} (130 M^{-1} s^{-1} for G and 200 M^{-1} s^{-1} for Z), whereas substitution at the 3′-position has little effect on ε_{350}. Oxidation potentials determined by square wave voltammetry (phosphate buffer, pH 7.4) for the nucleosides dZ, dG, dA, and dI are 0.80, 1.11, 1.36, and 1.52 V, respectively, versus Ag/Ag^+. Values for nucleosides G and A are similar to those reported for the nucleotides.[18]

Photodimerization. Solutions of the single-strand and hairpin systems (ca. 4 μM oligonucleotide) in aqueous buffer were irradiated at 280 nm, a wavelength at which thymine absorbs much more strongly than T<>T (Table S2). The progress of irradiation was monitored by HPLC with UV detection at 260 nm,

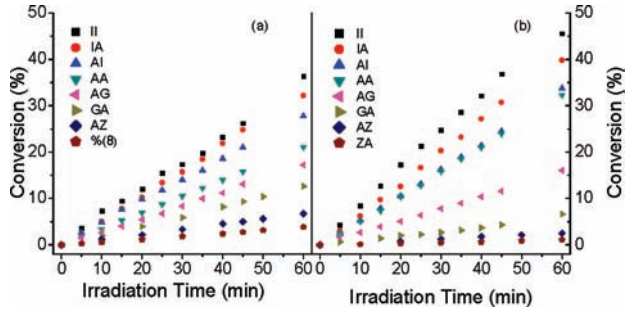

Figure 3. Conversion of starting material (see Chart 1 for structures) to products containing thymine vs 280 nm irradiation time: (a) single strands and (b) hairpins. Conversions determined by HPLC analysis for ca. 4 μM solutions of oligonucleotide in 10 mM phosphate buffer (pH 7.1) containing 100 mM NaCl.

the absorption maxima of both reactants and products (see Figure S4). A major product peak assigned to the *cis*−*syn* (2 + 2) dimer T<>T was observed in all cases, with minor peaks accounting for <5% of total product.[17,19] Plots of percent conversion of starting material to product versus irradiation time obtained from integrated HPLC peak areas are shown in Figure 3.

The initial slopes of the plots shown in Figure 3 are dependent upon both the choice of single-strand versus hairpin structure and the flanking purine, as reported in Table 1. These slopes can be converted to quantum yields (moles T<>T per moles light absorbed by TT) by correction of the HPLC data for differences in molar absorbance and for the percent of incident light absorbed by TT, using the molar absorbance of the individual bases at 260 and 280 nm, respectively (see Supporting Information, Tables S2 and S3). This correction assumes that the nonreactive bases are competitive absorbers of UV irradiation and that the base absorbance is not strongly influenced by the identity of flanking bases. The resulting values of Φ_{TT} are reported in Table 1 along with the yields for single-strand systems relative to AA_S and for duplex systems relative to AA_H (Φ_{TT} rel = 1.0). The Φ_{TT} trends are the same as those obtained from the uncorrected HPLC data (Figure 3). Thus, corrections for differences in UV absorbance serve to refine the data but do not alter the trends that are readily apparent in Figure 3.

Table 1. Slopes of Figure 3, Light Absorbed by TT, Absolute and Relative Quantum Yields for TT Dimerization[a]

	Figure 3 slope[b]	TT abs. %[c]	10^3 Φ_{TT}[d]	Φ_{TT} rel.[e]
II_S	0.44	44	2.4	1.7
IA_S	0.37	44	2.0	1.5
AI_S	0.36	44	1.9	1.4
AA_S	0.25	43	1.4	(1.0)
AG_S	0.20	36	0.85	0.63
GA_S	0.14	36	0.63	0.46
AZ_S	0.077	36	0.34	0.25
ZA_S	0.040	36	0.19	0.14
II_H	0.86	25	9.8	1.7
IA_H	0.63	25	7.2	1.2
AI_H	0.53	25	6.0	1.0
AA_H	0.52	25	5.8	(1.0)
AG_H	0.25	22	2.8	0.48
GA_H	0.096	22	1.1	0.19
GG_H	n.d.[f]	20	<0.1	
AZ_H	0.048	22	0.67	0.11
ZA_H	0.014	22	0.22	0.04
ZZ_H	n.d.[f]	20	<0.1	

[a] See Figure 3 caption for irradiation conditions. [b] Initial slopes of Figure 3 (% conversion/min). Estimated error ±5%. [c] Percentage of light absorbed by TT step at 280 nm obtained from molar absorbance coefficients (Table S2). Estimated error ±5%. [d] Quantum yield for the (2 + 2) thymine dimer formation corrected for competitive absorption at 280 nm and HPLC response (Table S3). Estimated cumulative error for measurement of light intensity and corrections for absorbance ±10%. [e] Quantum yields relative to values for AA_S (for single-stranded) or AA_H (for hairpins). [f] Yields too low for accurate determination.

DISCUSSION

Ground State Conformation. The structure and photochemical behavior of the parent single-strand and hairpin systems AA_S and AA_H have previously been investigated by our research groups.[9,14,17] The structures of AA_S and AA_H were also investigated by means of molecular dynamics simulation using the CHARMM force field.[17] Snapshots of conformations having stacked thymines are shown in Figure 4a and probability densities for the distances between centers of the C5−C6 bonds in the TT steps are shown in Figure 4b. The snapshot of AA_S shows a largely unstacked structure, other than the imposed TT stacking. The snapshot of AA_H shows a conformation with B-DNA geometry, in agreement with the solution NMR structure which was determined using ^{1}H NMR spectral data and constrained torsion angle molecular dynamics.[15] The central ATTA domain of this hairpin was found to adopt a normal B-DNA structure. The probability density for AA_H is approximately Gaussian with a maximum at 4.2 Å (Figure 4b), corresponding to the average distance between centers of C5−C6 bonds in a B-DNA TT step. The probability density for AA_S (Figure 4b) is broader and includes higher populations both at very short distances (assumed to be most reactive toward TT dimerization, Scheme 1) as well as longer distances, corresponding to unstacked single-strand structures. Setting a short cutoff for well-stacked ground state conformations (Scheme 1, d < 3.52 Å) results in similar populations of reactive conformations for single-strand and hairpin systems.[9] Both Johnson and Wiest[7] and Law et al.[8] set similar limits for d in their simulations of TT dimerization.

We now have investigated the pairwise interaction energies for TT with the 5′- or 3′-A in AA_S and AA_H (Figure 1). The probabilities of strong TT or AT dinucleotide interactions in AA_S are low and probabilities of ATT or TTA trinucleotide interactions are too low to be detected (Figure 1a,b). Low probabilities of strong pairwise interaction energies are indicative of the absence of significant populations of π-stacked ATT or TTA trinucleotide conformations within the hexanucleotide AA_S, as previously reported for the trinucleotides 5′-ATT and 5′-TTA.[20]

The calculated probabilities of strong interaction energies in the internal ATT and TTA trinucleotide sequences of AA_H are both high (Figure 1c,d). This is consistent with the well-stacked B-DNA structure for this hairpin obtained from ^{1}H NMR spectral analysis.[15] We note that the average interaction energy is somewhat lower for 3′- versus 5′-AT. The crystal structure for a duplex containing an ATTA sequence shows more extensive π-overlap for the 5′- versus 3′-AT. Stacked aromatics are known

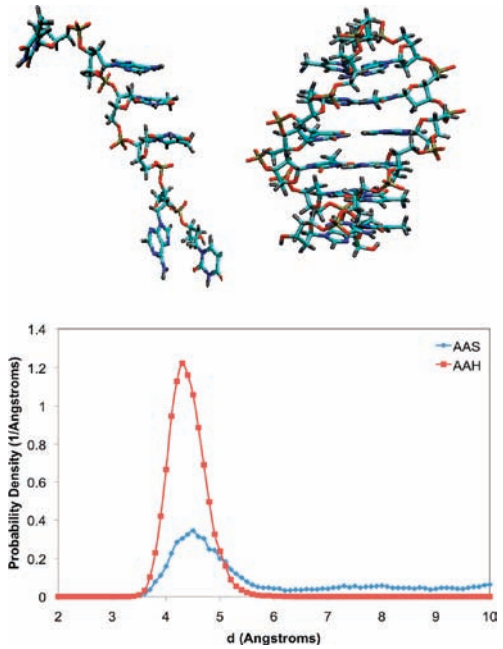

Figure 4. Snapshots of AA_S and AA_H having well-stacked TT conformations appropriate for TT dimerization and probability densities for the distance between centers of the C5−C6 bonds in the TT steps of AA_S and AA_H (reproduced from ref 17; copyright 2010 American Chemical Society).

to favor slipped versus sandwich geometries.[21] Increased π-overlap may lead to increased electrostatic repulsion between adjacent bases, thus, resulting in a higher average interaction energy for 5′- versus 3′-AT.

The melting temperatures of hairpins possessing G−C or Z−C base pairs are higher than those of AA_H and are essential independent of base pair 5′- versus 3′-location (Table S1). Values of T_m for hairpins possessing I−C base pairs are lower than the value for AA_H, as expected for a purine lacking one of the hydrogen bond donor groups present in G−C or Z−C base pairs.[22] All of the hairpins have T_m values well above the ambient temperatures used for photochemical experiments. Replacement of a flanking A−T base pair by a stronger G−C base pair might be expected to change the population of ground state conformers (Scheme 1). However, the probability densities for the distance *d* between TT double bonds obtained from molecular dynamics simulations for AA_H, AG_H, and GA_H are essentially identical (Figure S1).

Kundu et al.[11] suggested that an increase in duplex rigidity for a TT step with flanking G−C versus A−T base pairs might hinder the substantial duplex reorientation necessary to accommodate the photodimer. The crystal structure of a duplex containing a TT dimer with flanking adenines displays a 30° bend.[23] However, in view of the concerted, ultrafast formation of the TT dimer,[4,24] it is unlikely that product stability should influence the efficiency of dimer formation in a short, unconstrained duplex domain such as that in the hairpin AA_H. The strength of hydrogen bonding might, however, affect the ground state populations of reactive conformers.

Photodimerization Efficiency and Purine Ionization Potential. The use of monochromatic 280 nm light permits moderately selective excitation of T at a wavelength where the TT dimer does not absorb appreciably (Table S2). Thus, higher

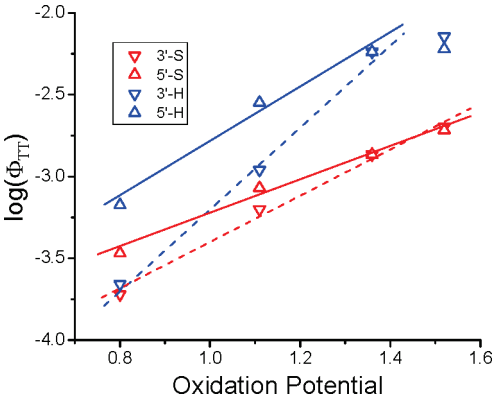

Figure 5. Correlation of $\log(\Phi_{TT})$ with purine oxidation potential (from left to right: 7-deazaguanine, guanine, adenine and inosine) for single-strand and hairpin systems. Single-strand and hairpin systems have a variable 3′ or 5′ purine with adenine in the other flanking position. Dashed and solid lines show correlations for 3′-purines and 5′-purines, respectively. Correlations exclude data for I-containing hairpins.

conversions of our single-strand and hairpin systems to dimer-containing products are realized than is possible with the shorter wavelength 254 nm excitation used in previous studies.[11,12] Conversion of the initial slopes of plots of conversion versus irradiation time (Figure 3) to quantum yields for TT dimer formation (Table 1) requires corrections of HPLC data for absorbance of reactants and products and for the percent absorbance of 280 nm irradiation by the TT step. The use of single base 280 nm absorption coefficients (Table S2) provides similar values for the %TT absorbance to those obtained from an online DNA UV calculator.[25] The %TT absorbance is larger for the systems containing the purines A and I versus G and Z, resulting in larger purine-dependence for the values of Φ_{TT} than provided by the initial slopes of Figure 3 (Table 1). The larger %TT absorbance for single-strand versus hairpin systems results in a smaller difference in the values of Φ_{TT} than indicated by the initial slopes of Figure 3 (Table 1). The values of Φ_{TT} for AA_S and AA_H are larger than our previously reported values which were not corrected for the absorbance of light by nonreactive bases.[17]

Plots of $\log(\Phi_{TT})$ versus purine oxidation potential for single-strand and hairpin systems having a variable 3′ or 5′ purine with adenine at the other flanking position are shown in Figure 5. Values of Φ_{TT} decrease as the ionization potential of the variable purine base decreases (I > A > G > Z) for both single-strand and duplex systems. Quenching by 5′-G and Z in the hairpins GA_H and ZA_H is particularly pronounced. Reasonably good linear fits (R^2 > 0.98) were obtained for single-strand systems and for hairpin systems (when the data for I is excluded). The diminished effect of I in the hairpin versus single-strand systems may be related to the low T_M for I-containing hairpins, which might reflect less ordered ground state conformations in the vicinity of the TT step.

Correlations of the TT dimer yield with the oxidation potential of the flanking purine have previously been ascribed to excited state electron transfer processes.[12,13] Holman et al. attributed the purine effect observed using 254 nm irradiation to purine-sensitized dimer repair.[12] By analogy to the extensively studied flavin repair mechanism,[26] electron transfer from the excited purine to the TT dimer was proposed to result in cleavage of the TT dimer anion radical.[12] The high conversions to dimer and linear nature of plots of yield versus irradiation

Scheme 2. Effect of a Flanking 5′-Purine (P) on TT Photodimerization

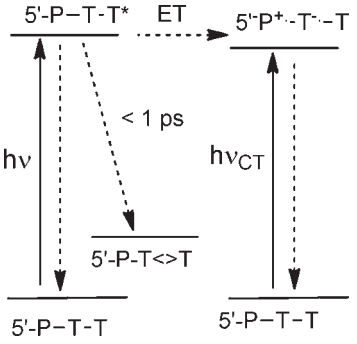

time for 280 nm irradiation (Figure 3) are inconsistent with a purine-sensitized repair mechanism under our conditions. Cannistraro and Taylor[13] noted that the purine effect that they observed for 302 nm irradiation of duplexes containing a T−^{m}C step (^{m}C = 5-methylcytosine) could not be the result of a purine-sensitized repair mechanism because of the absence of purine absorption at this wavelength. However, 313 nm excitation of a duplex possessing a TT dimer with a flanking 8-oxoguanine which is selectively excited at this wavelength was reported to effect dimer repair.[26]

Cannistraro and Taylor[13] proposed that the purine effect is a consequence of quenching of the pyrimidine excited state by the flanking purine via an electron transfer mechanism in which the pyrimidine serves as the electron acceptor and the purine as an electron donor (Scheme 2, ET). According to their proposed mechanism, excited state electron transfer results in the formation of an exciplex which decays to the ground state via nonradiative decay rather than exciplex fluorescence or TT dimer formation. The free energy for photoinduced electron transfer can be estimated using Weller's equation ($\Delta G_{ET} \sim (E_S - E_{rdn} + E_{ox})$[27] from the singlet energy of dT and reduction potential of dT (ca. 4.1 eV and −2.24 V vs Ag/Ag^{+},[28] respectively) and the oxidation potentials of dI, dA, dG, and dZ (Figure 5). The resulting values of ΔG_{ET} are consistent with electron transfer quenching of the thymine singlet state. Redox potentials are expected to be influenced by base pairing, π-stacking, and solvation; hence, these values should be viewed as approximate.

The higher values of Φ_{TT} for flanking I versus A indicate that A serves as a quencher of TT dimer formation, in agreement with the higher yields of dimerization observed for flanking pyrimidines T or C versus adenine,[6,13] both pyrimidines having higher oxidation potentials than adenine.[29] Quenching of TT dimerization by flanking A was not considered in applying our conformational model for TT dimerization to single-strand and hairpin systems including AA_S and AA_H.[9] Our model employs as benchmarks the dimerization quantum yields for $(dT)_{20}$ and $(dT)_{20}(dA)_{20}$, neither of which has purines flanking a TT step. The omission of purine quenching from our model could account for the somewhat higher calculated versus experimental values of Φ_{TT} for AA_S and AA_H.[17]

Photodimerization Efficiency and Purine Location. Values of Φ_{TT} are sensitive to the location of the flanking purine as well as its oxidation potential (Figure 5). Cannistraro and Taylor[13] proposed that more efficient quenching by 5′- versus 3′-purines reflects more extensive π-overlap of the flanking 5′-purine versus 3′-purine with the adjacent thymine. This proposal is consistent with the crystal structure of a duplex containing an ATTA sequence.[30] However, it does not account for the similar sensitivity of Φ_{TT} to the ionization of the flanking purine in single-strand systems (which have no detectable π-stacking with TT, Figure 1a,b) and the 3′-hairpin systems which have extensive π-stacking (Figure 1c,d). Thus, the extent of π-stacking alone does not account for the pronounced quenching of TT dimerization by 5′-G or Z in the hairpins GA_H and ZA_H.

An alternative explanation for more efficient quenching by 5′- versus 3′-purines is provided by the observation of much stronger long wavelength absorption for GA_H versus AG_H and ZA_H versus AZ_H (Figure 2). Banyasz et al.[31] have recently reported enhanced long-wavelength absorbance for $(dT)_{20}$, $(dA)_{20}$, and their duplex compared to those of the single nucleotides. They attribute these long-wavelength bands to charge-transfer (CT) absorption of the stacked bases. Our value for the molar absorption coefficient of AA_H at 350 nm (ε_{350}) is 76 M^{-1} cm^{-1} or 12 M^{-1} cm^{-1} per base pair, similar to the value/base reported by these workers for the duplex $(dA)_{20}\cdot(dT)_{20}$. Substitution of G or Z for A at the hairpin 5′-position results in larger increases in ε_{350} (132 and 198 M^{-1} cm^{-1}, respectively); whereas substitution at the hairpin 3′-position or in the 5′ or 3′ position of single-strand systems has little effect on ε_{350}. The dependence of ε_{350} on the 5′-purine oxidation potential has not been reported previously, but is consistent with the assignment of the long-wavelength bands of hairpins having 5′-A, G, or Z purines to the CT transition of a ground-state EDA complex.

Excitation of the EDA complex ($h\nu_{CT}$) is expected to result in direct formation of a charge-transfer stabilized exciplex, without competition from TT dimer formation (Scheme 2). Evaluation of the relative contributions of excited state and ground state pathways for electron transfer quenching of TT dimerization in the 5′-hairpin systems (Scheme 2) would require detailed information about the electronic excited states of these complex multichromophoric systems as well as their ground state conformations and thus is well beyond the scope of this study of dimerization efficiency. It should be borne in mind that it is the absorption of light by the reactive minority conformations and not the ensemble of ground state conformations that will determine dimerization efficiency.

The linear nature of the plots in Figure 5 for single-strand systems suggests that values of Φ_{TT} in these systems are determined by the competition between dimerization (k_{TT}) and exciplex formation (k_{ET}). Assuming a value of ca. 10^{12} s^{-1} for dimerization of a well-aligned TT step[3,4] and the absence of electron transfer quenching for II_S and II_H, values of $k_{ET} \sim 10^{13}$ s^{-1} can be estimated for quenching by 3′-Z from the relative quantum yields in Table 1, with somewhat lower values for quenching by 3′-G or 3′-A. These values are similar to those for electron-transfer quenching of the singlet states of arenedicarboxamide hairpin linkers by adjacent purines which follow a normal Marcus free energy dependence.[32] Evidently, the absence of ground state π-stacking in the single-strand systems has only a modest effect on electron transfer quenching dynamics.

■ CONCLUSION

Quantum yields for TT photodimerization in single-strand systems and base-paired hairpins containing flanking purines have been determined for the first time using HPLC data corrected for UV absorption of reactants and products (Table 1). The low values of Φ_{TT} indicate that ground state conformation is

the major determinant of dimerization efficiency. Values of Φ_{TT} are dependent upon both the ionization potential of the flanking base (I > A > G > Z) and its location. This dependence is attributed to a combination of excited state electron transfer quenching and, in the case of the 5′-hairpin systems, ground state EDA complex formation (Scheme 2). Both pathways lead to excited state complexes (exciplexes) which decay to the ground state, thus, reducing the efficiency of dimer formation. Evidence in support of EDA complex formation is provided by the appearance of weak long-wavelength absorption bands, which are most prominent for 5′-G and Z flanking bases (Figure 2). Absorption of UVA and UVB irradiation (290−400 nm) by the EDA complexes of adjacent purine and pyrimidine bases provides a potential mechanism for the protection of cellular DNA from UV damage. The importance of this pathway remains to be more fully elucidated.

■ ASSOCIATED CONTENT

Supporting Information. Experimental section with Tables containing m/z, T_M, and UV data and methods used for calculation of quantum yields. Figures showing UV spectra and typical HPLC data. This material is available free of charge via the Internet at http://pubs.acs.org.

■ AUTHOR INFORMATION

Corresponding Author

fdl@northwestern.edu; schatz@chem.northwestern.edu

Present Addresses

[†]School of Chemistry, Indian Institute of Science Education and Research, Thiruvananthapuram, Kerala, India 695016.

■ ACKNOWLEDGMENT

Funding for this project was provided by the National Science Foundation (NSF-CRC grant CHE-0628130).

■ REFERENCES

(1) (a) Taylor, J. S. *Acc. Chem. Res.* **1994**, *27*, 76. (b) Friedel, M. G.; Cichon, M. K.; Carell, T. In *Organic Photochemistry and Photobiology*; Horspool, W., Lenci, F., Eds.; CRC Press: Boca Raton, FL, 2004.

(2) (a) Beukers, R.; Berends, W. *Biochim. Biophys. Acta* **1960**, *41*, 550. (b) Cadet, J.; Vigny, P. In *The Photochemistry of Nucleic Acids*; Morrison, H.; Wiley: New York, 1990.

(3) Schreier, W. J.; Kubon, J.; Regner, N.; Haiser, K.; Schrader, T. E.; Zinth, W.; Clivio, P.; Gilch, P. *J. Am. Chem. Soc.* **2009**, *131*, 5038.

(4) Schreier, W. J.; Schrader, T. E.; Koller, F. O.; Gilch, P.; Crespo-Hernandez, C. E.; Swaminathan, V. N.; Carell, T.; Zinth, W.; Kohler, B. *Science* **2007**, *315*, 625.

(5) Johns, H. E.; Pearson, M. L.; Helleiner, C. W.; Leblanc, J. C. *J. Mol. Biol.* **1964**, *9*, 503.

(6) Douki, T.; Court, M.; Sauvaigo, S.; Odin, F.; Cadet, J. *J. Biol. Chem.* **2000**, *275*, 11678.

(7) Johnson, A. T.; Wiest, O. *J. Phys. Chem. B* **2007**, *111*, 14398.

(8) Law, Y. K.; Azadi, J.; Crespo-Hernandez, C. E.; Olmon, E.; Kohler, B. *Biophys. J.* **2008**, *94*, 3590.

(9) McCullagh, M.; Hariharan, M.; Lewis, F. D.; Markovitsi, D.; Douki, T.; Schatz, G. C. *J. Phys. Chem. B* **2010**, *114*, 5215.

(10) Becker, M. M.; Wang, Z. *J. Mol. Biol.* **1989**, *210*, 429. Bourre, F.; Renault, G.; Seawell, P. C.; Sarasin, A. *Biochimie* **1985**, *67*, 293.

(11) Kundu, L. M.; Linne, U.; Marahiel, M.; Carell, T. *Chem.—Eur. J.* **2004**, *10*, 5697.

(12) Holman, M. R.; Ito, T.; Rokita, S. E. *J. Am. Chem. Soc.* **2007**, *129*, 6.

(13) Cannistraro, V. J.; Taylor, J. S. *J. Mol. Biol.* **2009**, *392*, 1145.

(14) Hariharan, M.; Lewis, F. D. *J. Am. Chem. Soc.* **2008**, *130*, 11870.

(15) Siegmund, K.; Hariharan, M.; Lewis, F. D. *J. Phys. Chem. B* **2011**, *115*, 3740.

(16) Foloppe, N.; MacKerell, A. D. *J. Comput. Chem.* **2000**, *21*, 86.

(17) Hariharan, M.; McCullagh, M.; Schatz, G. C.; Lewis, F. D. *J. Am. Chem. Soc.* **2010**, *132*, 12856.

(18) (a) Oliveira-Brett, A. M.; Piedade, J. A. P.; Silva, L. A.; Diculescu, V. C. *Anal. Biochem.* **2004**, *332*, 321. (b) Stempkowska, I.; Liga, M.; Jasnowska, J.; Langer, J.; Filipiak, M. *Bioelectrochemistry* **2007**, *70*, 488.

(19) Low yields of minor products have previously been reported for AA_S and AA_H.[17]

(20) Pan, Z.; McCullagh, M.; Schatz, G. C.; Lewis, F. D. *J. Phys. Chem. Lett.* **2011**, *2*, 1432.

(21) Sherrill, C. D.; Sinnokrot, M. O. *J. Am. Chem. Soc.* **2004**, *126*, 7690.

(22) Watkins, N. E.; SantaLucia, J. *Nucleic Acids Res.* **2005**, *33*, 6258.

(23) Park, H.; Zhang, K.; Ren, Y.; Nadji, S.; Sinha, N.; Taylor, J. S.; Kang, C. *Proc. Natl. Acad. Sci. U.S.A.* **2002**, *99*, 15965.

(24) Boggio-Pasqua, M.; Groenhof, G.; Schaefer, L. V.; Grubmueller, H.; Robb, M. A. *J. Am. Chem. Soc.* **2007**, *129*, 10996.

(25) Tataurov, A. V.; You, Y.; Owczarzy, R. *Biophys.Chem.* **2008**, *133*, 66.

(26) Nguyen, K. V.; Burrows, C. J. *J. Am. Chem. Soc.* 2011, *133*, 14586.

(27) Weller, A. *Z. Phys. Chem. Neue Folge* **1982**, *133*, 93.

(28) The singlet energy can be estimated from the crossing points of the fluorescence and fluorescence excitation (or absorption) spectra; Markovitsi, D.; Onidas, D.; Gustavsson, T.; Talbot, F.; Lazzarotto, E. *J. Am. Chem. Soc.* **2005**, *127*, 17130.

(29) Seidel, C. A. M.; Schulz, A.; Sauer, M. H. M. *J. Phys. Chem.* **1996**, *100*, 5541.

(30) Quintana, J. R.; Grzeskowiak, K.; Yanagi, K.; Dickerson, R. E. *J. Mol. Biol.* **1992**, *225*, 379.

(31) Banyasz, A.; Vaya, I.; Changenet-Barret, P.; Gustavsson, T.; Douki, T.; Markovitsi, D. *J. Am. Chem. Soc.* **2011**, *133*, 5163.

(32) Lewis, F. D.; Kalgutkar, R. S.; Wu, Y.; Liu, X.; Liu, J.; Hayes, R. T.; Wasielewski, M. R. *J. Am. Chem. Soc.* **2000**, *122*, 12346.